Equilibrium temperature in intrinsic hydrogenated amorphous silicon under illumination

S. Vignoli, R. Meaudre, and M. Meaudre
Département de Physique des Matériaux, Université Claude Bernard Lyon I, 43 boulevard du 11 Novembre 1918, 69622 Villeurbanne Cédex, France
(Received 9 May 1994)

The influence of illumination on the thermal equilibrium temperature of the defect structure in undoped a-Si:H has been studied by measurements of the defect density versus temperature up to 290 °C. It was found that the light-induced excess carrier concentration leads to a decrease of the thermal equilibrium temperature depending on the carrier generation rate. This behavior is consistent qualitatively as well as quantitatively with a phenomenological model recently developed over a wide range of carrier generation rates.

I. INTRODUCTION

It is now well established that the defect density in extrinsic or intrinsic hydrogenated amorphous silicon can reach equilibrium above a temperature denoted T_E.[1,2] That means that above T_E the defect density is temperature dependent and below T_E it depends on the prior thermal history of the sample and slowly relaxes towards equilibrium with a relaxation time τ which is thermally activated[2] and which has been shown to be correlated with hydrogen diffusion.[3]

Recently it has been shown that illuminating the sample during isothermal relaxation towards equilibrium after defect creation by thermal quenching or strong illumination enhances the annealing rate of defects.[4-7] These works are of major importance in order to understand the light-induced metastability phenomena and the apparent saturation of the defect density which is widely observed.[8-11] They have been explained in the light of an enhancement of the hydrogen diffusion processes as predicted by theoretical studies[12] and by exodiffusion spectra.[13]

Since the equilibrium temperature of the defect density T_E is related to τ, we expect a decrease of T_E under illumination. This is precisely what we report in this paper by measurements of the defect density in the dark and under illumination versus temperature up to 290 °C, and the experimental results are discussed in the light of a phenomenological model recently developed.[14,15]

II. SAMPLES AND EXPERIMENTAL PROCEDURE

The undoped 0.9-μm-thick a-Si:H films were deposited by rf glow discharge from pure silane at 250 °C in a hot-wall multiplasma monochamber reactor.[16] For coplanar dark conductivity σ_d and photoconductivity σ_{ph} measurements, two strips of chromium separated by about 1 mm were evaporated after film deposition.

The light source used was a halogen lamp with a 10-cm-thick water filter in order to cut the infrared part of the spectrum. A generation rate G as high as 6×10^{21} $\text{cm}^{-3}\,\text{s}^{-1}$ can then be obtained and could be lowered by neutral filters to avoid modifications of the spectrum.

All thermal treatments and measurements were made in vacuum (10^{-6} Torr). Defect densities N were determined by the integration of the excess subgap absorption measured at 30 °C by the CPM (constant photocurrent method) using a conversion factor of 1.9×10^{16} $\text{cm}^{-2}\,\text{eV}^{-1}$.[17] In the annealed state one has typically $N_0=5\times10^{15}\,\text{cm}^{-3}$.

Prior to each measurement, the sample was annealed in the dark at 250 °C for 1 h. Dark-conductivity–temperature characteristics were recorded as the sample was warming up to 250 °C (at a rate of 0.02 °C s^{-1}) after a slow cooling or a thermal quenching to room temperature (cooling rates being 0.04 °C s^{-1} and 10 °C s^{-1}, respectively), whereas photoconductivity-temperature characteristics were recorded during the slow cooling from 250 °C.

For isothermal relaxation experiments the time dependence of the dark conductivity was measured at different temperatures T after annealing 15 min at 290 °C and quenching to room temperature and then rapidly warming up to T. The relaxation was then observed, defining $t=0$ to be the moment that the temperature of the film stabilized at T.

III. EXPERIMENTAL RESULTS

A. Dark equilibrium temperature

Figure 1 shows the Arrhenius plot of the dark conductivity after quenching from 290 °C and slow cooling. We clearly observe the two behaviors separated by T_E, the dark equilibrium temperature, that means the electronic properties are independent and dependent on the prior thermal history of the sample above and below T_E, respectively. From this plot we find $T_E=230$ °C in good agreement with the values usually found in the range 190 °C–230 °C.[2,18-21]

So, in order to confirm this value of T_E, we have performed dark isothermal relaxation at different temperatures. In Fig. 2 we have plotted the normalized time dependence of $\sigma_d(t)$:

$$Y(t)=[\sigma_d(t)-\sigma_{df}]/[\sigma_d(0)-\sigma_{df}] ,$$

 ©1994 The American Physical Society

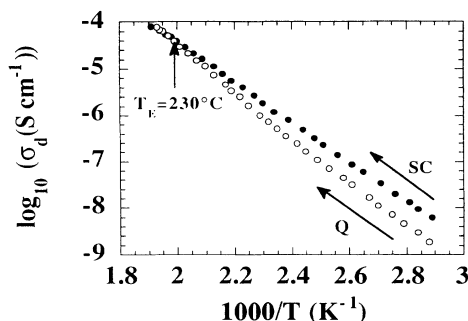

FIG. 1. Arrhenius plots of the dark conductivity after quenching (Q) and slow cooling (SC). The vertical arrow indicates the thermal equilibrium temperature in the dark (T_E).

where $\sigma_d(0)$ is the dark conductivity at the beginning of the relaxation and σ_{df} the final steady-state value of $\sigma_d(t)$. Figure 2 shows that the evolution of $\sigma_d(t)$ is not a simple exponential but is well described by a stretched exponential function $\exp[-(t/\tau)^{\beta}]$. The values of τ and β for the different temperatures are reported in Fig. 2.

The relaxation times τ derived from our measurements have been plotted in Fig. 3 as a function of reciprocal temperature. It is shown that τ is thermally activated with an activation energy of 1.5 eV, as already quoted for undoped *a*-Si:H[2]. The extrapolation of the solid curve in Fig. 3 gives $\tau \cong 40$ s at 230 °C. Since T_E is the temperature at which the electronic properties come into equilibrium in a few seconds, this result strongly confirms our value of the dark equilibrium temperature derived from Fig. 1.

Figure 4 shows the variations of the defect density with the inverse temperature. The data represented by the open circles were obtained as follows: the samples were first annealed 1 h at 250 °C, then slowly cooled to room temperature, and finally rapidly (typically, 5–10 min) warmed up to T before quenching to room temperature to avoid any relaxation of the samples. Data symbolized by solid circles were obtained after complete dark isothermal relaxation at different temperatures. Then the dashed curve in Fig. 4 represents the defect density at equilibrium in the dark $N_{eq}(T)$ which is thermally activated by 0.2 eV, as has been widely observed (for a review, see Ref. 14). So these results directly confirm that

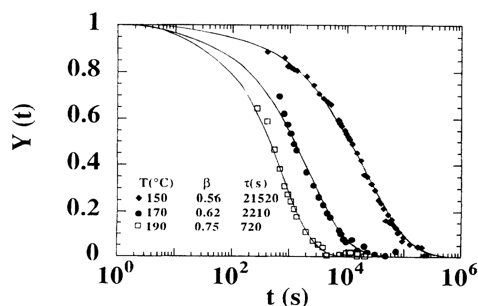

FIG. 2. Time dependence of the normalized reduced conductivity at different temperatures. The solid curves are fitted to the data using the stretched exponential function $\exp[-(t/\tau)^{\beta}]$, and β and τ values given in the figure.

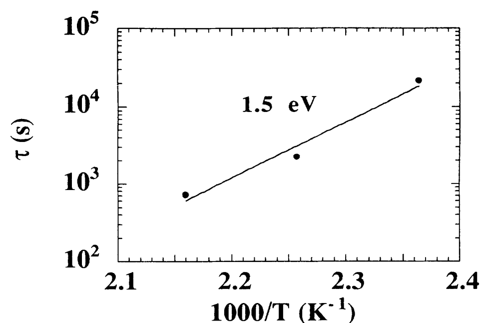

FIG. 3. Values of the relaxation time τ given in Fig. 2 vs reciprocal temperature. The solid curve is fitted to the data.

above about 230 °C, the defect structure is in thermal equilibrium and the fact that a direct link exists between electronic properties (or dark conductivity) and defect concentration.[2]

B. Equilibrium temperature under illumination

In order to evaluate an eventual change of the equilibrium temperature when the sample is illuminated due to the increase of carrier density, we have performed two kinds of measurements. The first one consists in a slow cooling under illumination (at the same rate as in the dark) from 250 °C down to T where the light is switched off and the samples are immediately quenched to room temperature. Hereafter, these measurements will be referred to as SCL (slow cooling under light) measurements.

The second type of measurement we carried out consists in illuminating the annealed samples at a given temperature during 1 min after which quenching to room temperature was performed. Hereafter, these measurements will be referred to as 1M measurements. Note that, for both kinds of experiments, between two measurements, the sample was annealed 1 h at 250 °C and then slowly cooled down to room temperature in order to check the reversibility and to start each measurement from the same annealed state.

Figure 5 shows plots of the defect density versus inverse temperature obtained with SCL measurements (solid circles) and with 1M measurements (open circles) for three carrier generation rates:

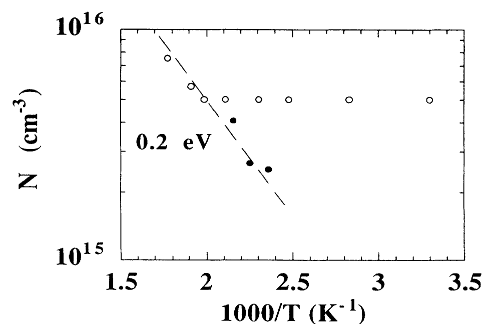

FIG. 4. Defect density in the dark as a function of reciprocal temperature. The dashed curve represents the thermal equilibrium defect density (for details see the text).

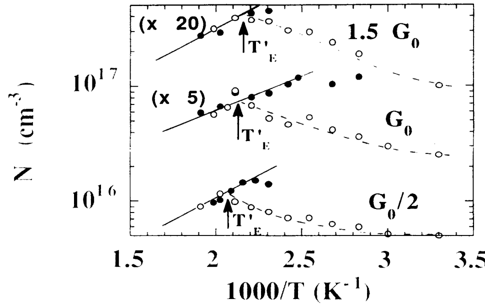

FIG. 5. Defect density under illumination for different carrier generation rates vs reciprocal temperature. The dashed curves are guides to the eye and the solid curves represent the thermal equilibrium defect density under illumination. The arrows indicate the thermal equilibrium temperatures under illumination. Note that the data for $G=G_0=4\times10^{21}$ cm^{-3} s^{-1} and $1.5G_0$ have been shifted as indicated for clarity (for details see the text).

$$G_0=4\times10^{21}\ \text{cm}^{-3}\,\text{s}^{-1}\ ,$$

$$1.5G_0,$$

and

$$G_0/2\ .$$

For clarity we have shifted the data for G_0 by a factor 5 and for $1.5G_0$ by a factor 20. These data show that, with both methods, the same defect density, which means the same state, is obtained for temperatures lower than the dark thermal equilibrium temperature. In other words, under illumination, thermal equilibrium is attained for temperatures T'_E lower than in the dark. The decrease in the thermal equilibrium temperature depends on the carrier generation rate, as we can see in Fig. 5, and T'_E is equal to about 190 °C, 200 °C, and 210 °C for $1.5G_0$, G_0, and $G_0/2$, respectively.

IV. DISCUSSION

A. Equilibrium temperature under illumination

Recently we have developed a phenomenological model for the time rate of change of the defect density $N(T,t)$ to render an account of a variety of experimental results.[14] This model assumes, for the creation of defects, a bimolecular process, as originally proposed by Stutzmann, Jackson, and Tsai,[22] and for the annealing of defects, a monomolecular process. In a recent paper we have been able to remove the ambiguity concerning the type of carrier that drives the annealing mechanism.[15]

So the basic equation in its dispersive version is

$$\frac{\partial N(T,t)}{\partial t}=(t/\theta)^{\beta-1}[c_d(T)n(T,t)p(T,t)-\lambda(T)N(T,t)p(T,t)]\ , \quad (1)$$

where $n(T,t)$ and $p(T,t)$ are the carrier densities in extended and shallow band-tail states and $c_d(T)$ and $\lambda(T)$ are two temperature-dependent parameters defining the ability of creating and annealing defects, respectively. $\beta\le1$ and θ characterize the dispersive behavior of the process.

So the relaxation time τ of isothermal relaxation is given by

$$\tau(T)=\left[\frac{\beta\theta^{\beta-1}}{\lambda(T)p(T)}\right]^{1/\beta}\ . \quad (2)$$

Then when the carrier concentration is increased, τ decreases and, therefore, the annealing rate increases or, in other words, the thermal equilibrium temperature decreases. This behavior was observed under illumination[4–7] and under low injection in pin devices.[23]

To quantify the shift of the thermal equilibrium temperature, we can write

$$\tau(T_E)=\tau(T'_E)\ , \quad (3)$$

T_E and T'_E being the thermal equilibrium temperatures in the dark and under illumination, respectively.

Providing β varies little with temperature, Eqs. (2) and (3) lead to

$$\lambda_0\exp\left[-\frac{E_1}{kT_E}\right]p_0(T_E)\cong\lambda_0\exp\left[-\frac{E_1}{kT'_E}\right]p(T'_E)\ , \quad (4)$$

where $p_0(T_E)$ and $p(T'_E)$ are the hole densities in the dark at T_E and under illumination at T'_E, respectively, and λ_0 and E_1 are the preexponential factor and the activation energy of $\lambda(T)$, respectively.

Now in order to estimate the ratio between $p_0(T_E)$ and $p(T'_E)$, we assume exponential density of states for both band tails and step functions for the density of states in valence and conduction bands, which means

$$N_{vbt}(E)=N_{v0}\exp\left[-\frac{E-E_v}{kT_v}\right]\quad \text{for } E\ge E_V\ , \quad (5a)$$

$$N_{cbt}(E)=N_{c0}\exp\left[\frac{E-E_c}{kT_c}\right]\quad \text{for } E\le E_C\ , \quad (5b)$$

and

$$N_{vb}(E)=N_{v0}\quad \text{for } E\le E_V\ , \quad (6a)$$

$$N_{cb}(E)=N_{c0}\quad \text{for } E\ge E_C\ , \quad (6b)$$

N_{c0} and N_{v0} being the densities of states at the mobility edges and kT_c and kT_v being the slopes of the conduction and valence band tails, respectively.

In our temperature range where thermal equilibrium proceeds, we can use the Boltzmann approximation to determine the ratios between band tail and free carriers and then we get in the dark,

$$\frac{p_{0bt}}{p_{0\text{free}}}=\frac{T_v}{T_v-T}\times\left\{\exp\left[\left[\frac{E_{\max}-E_v}{k}\right]\left[\frac{T_v-T}{T_vT}\right]\right]-1\right\}\ , \quad (7a)$$

$$\frac{n_{0bt}}{n_{0\text{free}}}=\frac{T_c}{T-T_c}\times\left\{1-\exp\left[\left[\frac{E_{\min}-E_c}{k}\right]\left[\frac{T-T_c}{TT_c}\right]\right]\right\}, \quad (7b)$$

where $E_{\max}$ ($E_{\min}$) is the energy level beyond (below) which holes (electrons) are considered as deeply trapped. Now, to determine the ratio between free electron and free hole densities, we assume that E_C-E_F is equal to the activation energy of the dark conductivity $E_a=0.86$ eV from the plot of Fig. 1. Taking $E_C-E_{\min}=0.2$ eV, $E_{\max}-E_V=0.3$ eV,[24] $kT_v=55$ meV from CPM spectra, $kT_c=26$ meV, and $E_g=1.8$ eV for the mobility gap, and since $N_{c0}=N_{v0}$, it is immediately seen that around 200 °C in the dark one has

$$n_{0bt}+n_{0\text{free}}\cong p_{0bt}+p_{0\text{free}} .$$

Under strong illumination one has $n\cong p$; then we get

$$\frac{n(T_E')}{n_0(T_E)}\simeq\frac{p(T_E')}{p_0(T_E)} . \quad (8)$$

From Eq. (1) the steady-state (equilibrium) defect density $N_{\text{eq}}(T)$ in the dark or under illumination is given by

$$N_{\text{eq}}(T)=\frac{c_d(T)n(T)}{\lambda(T)} . \quad (9)$$

So, combining Eqs. (8) and (9), we get

$$\frac{p(T_E')}{p_0(T_E)}=\frac{\lambda(T_E')N_{\text{eq}}(T_E')c_d(T_E)}{\lambda(T_E)N_{\text{eq}}(T_E)c_d(T_E')} , \quad (10)$$

where $N_{\text{eq}}(T_E)$ and $N_{\text{eq}}(T_E')$ are the equilibrium defect densities in the dark at T_E and under illumination at T_E', respectively.

Now, using Eq. (4), the thermal equilibrium temperature T_E' is given by

$$\frac{1}{T_E'}=\frac{1}{T_E}+\frac{k}{2E_2-E_1}\ln\left[\frac{N_{\text{eq}}(T_E')}{N_{\text{eq}}(T_E)}\right] , \quad (11)$$

where E_2 is the activation energy of $c_d(T)=c_{d0}\exp(-E_2/kT)$.

With $E_1=0.4$–0.5 eV (Refs. 15 and 25) and $E_2=0.1$ eV (Refs. 22 and 25) and taking the experimental values for $N_{\text{eq}}(T_E)$ and $N_{\text{eq}}(T_E')$, we find $T_E'=190$ °C–197 °C for $G=1.5G_0$, $T_E'=195$ °C–202 °C for $G=G_0$, and $T_E'=207$ °C–212 °C for $G=G_0/2$, in excellent agreement with the values found experimentally.

We note from Eq. (1) that the equilibrium defect density under illumination should vary as

$$N_{\text{eq}}(T)\propto\exp[-(E_2-E_1+E_3)/kT] ,$$

with E_3 the photoconductivity activation energy of about 0.2 eV, as deduced from the Arrhenius plots of σ_{ph} reported in Fig. 6. With the values of E_1 and E_2 given previously, we get

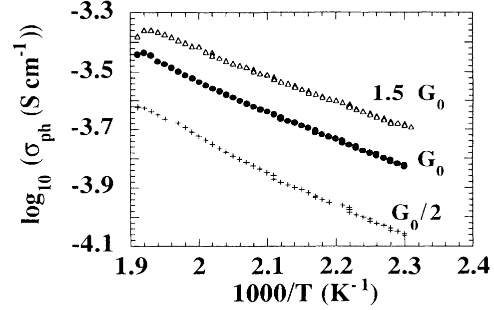

FIG. 6. Arrhenius plots of the photoconductivity for different carrier generation rates measured during slow cooling from 250 °C ($G_0=4\times10^{21}$ cm^{-3} s^{-1}).

$$N_{\text{eq}}(T)\propto\exp\left[\frac{x}{kT}\right] , \quad (12)$$

with 0.1 eV $\le x\le 0.2$ eV, here again in excellent agreement with the variations found experimentally in this work in the range 0.12–0.16 eV (see Fig. 5) as well as by other authors.[22,26,27]

Let us recall that the solid circles in Fig. 5 were obtained after slow cooling under illumination down to a temperature T followed by a quench to room temperature. The data which deviate from the straight lines simply mean that in the low-temperature range the samples did not have time enough to reach equilibrium during the slow cooling.

B. Equilibrium temperature versus carrier generation rate

Different groups have studied the kinetics of defect creation under strong illumination for different temperatures until saturation of the defect density (in fact, a balance between creation and annealing of defects) in undoped a-Si:H as well as in pin devices.[9,27,28] In Fig. 7 we have plotted the times t_{sat} at which saturation appears as a function of the reciprocal temperature for different carrier generation rates. Figure 7 shows that t_{sat} is thermally activated, as expected. Then, by extrapolating the solid curves in Fig. 7, we can deduce T_E' providing that at

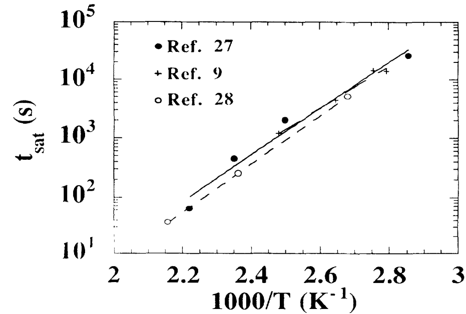

FIG. 7. Plots of the time required for the defect density to reach saturation t_{sat} at different carrier generation rates measured by different groups (Refs. 9, 27, and 28) vs reciprocal temperature. The curves are fitted to the data.

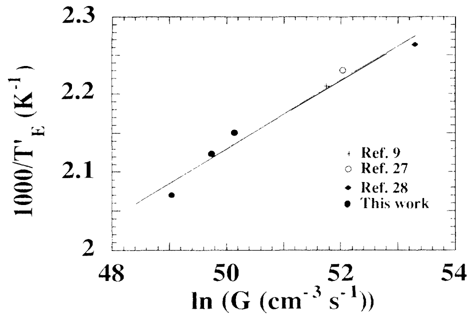

FIG. 8. Values of $1000/T'_E$ deduced from Figs. 5 and 7 (see the text) vs $\ln(G)$. The solid curve is a linear fit to the data.

T'_E, one has $t_{sat} \cong 100$ s and that degradation in pin devices is essentially due to the defect creation in the i layer.[29]

Now in Fig. 8 we have plotted the values of $1000/T'_E$ found in this work as well as the values deduced from Fig. 7 versus $\ln(G)$. We found a linear dependence between these two quantities, as shown in Fig. 8 by the solid curve, with a slope of about 5×10^{-2} K^{-1}. Since N_{eq} should vary as G^{γ}, with γ in the range $\frac{1}{3}-\frac{1}{2}$, as deduced from Fig. 5 and by other groups,[8,10] and combining with Eq. (11), it is easily shown that $1000/T'_E$ should vary linearly with $\ln(G)$ with a slope y given by

$$y=\frac{\gamma k}{2E_2-E_1}, \tag{13}$$

and with the values quoted above, we expect a slope in the range 3.2×10^{-2}–6.2×10^{-2} K^{-1} in good agreement with the experimental value.

V. CONCLUSION

Starting from undoped a-Si:H samples having a thermal equilibrium temperature T_E of about 230 °C in the dark, we have shown that white light illumination decreases T_E which, for example, reaches a value of about 190 °C for a carrier generation rate of 6×10^{21} $cm^{-3}\,s^{-1}$. These values are in good agreement with a phenomenological model which includes light-induced annealing of defects and with results obtained by other groups. Although in qualitative agreement with a mechanism according to which hydrogen diffusion is enhanced by illumination, these experiments, as well as hydrogen diffusion under illumination, must be pursued since, to our knowledge, a direct relationship between hydrogen diffusion and defect creation or annealing mechanisms is still missing.[30]

ACKNOWLEDGMENTS

The authors are indebted to P. Roca i Cabarrocas for providing a-Si:H samples. This work was partially supported by European Communities (JOULE II), ECOTECH/PIRSEM, and ADEME contracts. The Département de Physique des Matériaux is Unité de Recherche Associée No. 172 du CNRS.

[1]R. A. Street, *Hydrogenated Amorphous Silicon* (Cambridge University Press, Cambridge, England, 1991), p. 169.
[2]M. Meaudre, P. Jensen, and R. Meaudre, Philos. Mag. B **63**, 815 (1991).
[3]R. A. Street and K. Winer, Phys. Rev. B **40**, 6236 (1989).
[4]R. Meaudre and M. Meaudre, Phys. Rev. B **45**, 12 134 (1992).
[5]M. Isomura and S. Wagner, in *Amorphous Silicon Technology*, edited by M. J. Thomson, Y. Hamawaka, P. G. Le Comber, A. Madan, and E. Schiff, MRS Symposia Proceedings No. 258 (Materials Research Society, Pittsburgh, 1992), p. 473.
[6]H. Gleskova, P. A. Morin, and S. Wagner, Appl. Phys. Lett. **62**, 2063 (1993).
[7]C. F. O. Graeff, R. Buhleier, and M. Stutzmann, Appl. Phys. Lett. **62**, 3001 (1993).
[8]Z. Y. Wu, J. M. Siefert, and B. Equer, J. Non-Cryst. Solids **137-138**, 227 (1991).
[9]M. Isomura, N. Hata, and S. Wagner, Jpn. J. Appl. Phys. **31**, 3500 (1992).
[10]N. Hata, G. Ganguly, and A. Matsuda, Appl. Phys. Lett. **62**, 1791 (1993).
[11]S. Vignoli, R. Meaudre, M. Meaudre, and P. Roca i Cabarrocas, J. Non-Cryst. Solids **164-166**, 191 (1993).
[12]G. Müller, Appl. Phys. A **45**, 41 (1988).
[13]R. Weil, A. Busso, and W. Beyer, Appl. Phys. Lett. **53**, 2477 (1988).
[14]R. Meaudre, Solid State Commun. **89**, 239 (1994).
[15]R. Meaudre, S. Vignoli, and M. Meaudre, Philos. Mag. Lett. **69**, 327 (1994).
[16]R. Roca i Cabarrocas, J. P. Chevrier, J. Huc, A. Lloret, J. Y. Paret, and J. P. M. Schmitt, J. Vac. Sci. Technol. A **9**, 2331 (1991).
[17]Z. E. Smith, V. Chu, K. Shepard, S. Aljishi, D. Slobodin, J. Kolodzey, S. Wagner, and T. L. Chu, Appl. Phys. Lett. **50**, 1521 (1987).
[18]T. J. McMahon and R. Tsu, Appl. Phys. Lett. **51**, 412 (1987).
[19]X. Xu, M. Isomura, J. H. Yoon, S. Wagner, and J. R. Abelson, in *Amorphous Silicon Technology*, edited by A. Madan, Y. Hamawaka, M. J. Thomson, P. C. Taylor, and P. G. LeComber, MRS Symposia Proceedings No. 219 (Materials Research Society, Pittsburgh, 1991), p. 69.
[20]Z. E. Smith, S. Aljishi, D. Slobodin, V. Chu, S. Wagner, P. M. Lenahan, R. R. Arya, and M. S. Bennett, Phys. Rev. Lett. **57**, 2450 (1986).
[21]M. Vanecek, J. Fric, R. S. Crandall, and A. H. Mahan, J. Non-Cryst. Solids **164-166**, 335 (1993).
[22]M. Stutzmann, W. B. Jackson, and C. C. Tsai, Phys. Rev. B **32**, 23 (1985).
[23]R. A. Street, Appl. Phys. Lett. **59**, 1084 (1991).
[24]M. Stutzmann, Philos. Mag. B **56**, 63 (1987).
[25]R. Meaudre, M. Meaudre, and S. Vignoli, Phys. Rev. B **49**, 1716 (1994).
[26]L. E. Benatar, M. Grimbergen, D. Redfield, and R. H. Bube, in *Amorphous Silicon Technology* (Ref. 19), p. 117.
[27]P. V. Santos, W. B. Jackson, and R. A. Street, Phys. Rev. B

44, 12 800 (1991).
[28]L. F. Chen and L. Yang, J. Non-Cryst. Solids **137-138**, 1185 (1991).
[29]J. Hou, S. Bae, J. K. Arch, S. J. Fonash, M. Bennett, and L. F. Chen, in *Proceedings of the 11th PSEC, Montreux, 1992,* edited by L. Guimaraes, W. Palz, C. De Reyff, H. Kiess, and P. Helm (Harwood Academic, Chur, Switzerland, 1993).
[30]P. V. Santos, M. S. Brandt, R. A. Street, and M. Stutzmann, J. Non-Cryst. Solids **164-166**, 273 (1993).